Inorg. Chem. **2001,** *40,* 5162−5168

Preparation and Substitution Chemistry of $[Bu_4N]_2[W_6Cl_8(p\text{-}OSO_2C_6H_4CH_3)_6]$. A Useful Precursor for Pseudohalide, Acetate, and Organometallic Complexes Containing the $\{W_6Cl_8\}^{4+}$ Core

Charles S. Weinert, Nicholas Prokopuk, Stephanie M. Arendt, Charlotte L. Stern, and Duward F. Shriver*

Department of Chemistry, Northwestern University, 2145 Sheridan Road, Evanston Illinois 60208-3113

Received December 29, 2000

The tosylate (*p*-toluenesulfonate) cluster $[Bu_4N]_2[W_6Cl_8(p\text{-}OSO_2C_6H_4CH_3)_6]$ (**1**) has been prepared and characterized by IR and NMR spectroscopy, elemental analysis, and an X-ray crystal structure. This cluster complex is shown to be a useful starting material for the preparation of pseudohalide clusters, $[Bu_4N]_2[W_6Cl_8(NCQ)_6]$ (Q = O (**2**), S (**3**), and Se (**4**)), in high yields. Cluster **1** also serves as a precursor to the new cluster commpounds: $[Bu_4N]_2[W_6Cl_8(O_2CCH_3)_6]$ (**5**), $[Bu_4N]_2[W_6Cl_8\{(\mu\text{-}NC)Mn(CO)_2(C_5H_5)\}_6]$ (**6**), $[W_6Cl_8\{(\mu\text{-}NC)Ru(PPh_3)_2(C_5H_5)\}_6][p\text{-}OSO_2C_6H_4CH_3]_4$ (**7**), and $[W_6Cl_8\{(\mu\text{-}NC)Os(PPh_3)_2(C_5H_5)\}_6][p\text{-}OSO_2C_6H_4CH_3]_4$ (**8**). X-ray crystal structures are reported for **1**, **4,** and **5**.

Introduction

The group 5 and 6 metal halide clusters $[M_6Y_{12}X_6]^{n-}$ (M = Nb or Ta; X = Y = Cl, Br, or I) and $[M_6Y_8X_6]^{n-}$ (M = Mo or W; X = Y = Cl, Br, or I) have been the focus of recent research.[1] These materials are structurally related to the superconducting Chevrel phases[2,3] and typically exhibit interesting electrochemical and photophysical properties. For example, clusters of the type $[Ta_6Cl_8X_6]^{n-}$ exhibit up to five electrochemically accessible oxidation states,[4] and $[Mo_6Cl_8Cl_6]^{2-}$ has an unusually long-lived excited state.[5] These complexes contain a substitutionally inert inner core, $\{M_6Y_{12}\}^{n+}$ or $\{M_6Y_8\}^{n+}$ (Y = halide), surrounded by six axial ligands. The axial ligands can be terminal or bridging, giving discrete clusters or extended arrays of clusters, respectively. Recently, new extended arrays of these materials have been generated by introducing a variety of axial ligands to link the cluster core units through covalent or hydrogen bonding.[6−10]

The axial ligands, X, in discrete group 5 or 6 metal halide clusters are more labile than the inner ligands, Y. In addition, replacement of the halide ligands by more weakly coordinating ligands enhances ligand substitution. Ligands such as triflate,[11−16] perchlorate,[17] nitrate,[18−20] tetrafluoroborate,[19,21−24] alcohols,[25] and solvent molecules[26] have been employed for this purpose. The triflate ligand is attractive for this purpose because its coordination to the cluster core can be conveniently monitored by IR spectroscopy;[14,27] also triflate lacks the treacherous explosive properties of perchlorate in the presence of low-oxidation-state metals. The triflate ligand has been used extensively in our group to develop the substitution chemistry of niobium-,[11] tantalum-,[4,12] and molybdenum-containing[9,13,14,28,29] clusters.

For example, the cluster $[Bu_4N]_2[W_6Cl_8(OSO_2CF_3)_6]$ can be used to synthesize $[Bu_4N]_2[W_6Cl_8X_6]$ (X = F^-, Cl^-, Br^{--}, I^-, NCO^-, NCS^-, or $NCSe^-$) and $[W_6Cl_8(O{=}PPh_3)_6][OSO_2CF_3]_4$.[15,16] The substitution chemistry of this material is limited

---

* To whom correspondence should be addressed.

(1) Prokopuk, N.; Shriver, D. F. *Adv. Inorg. Chem.* **1999**, *46*, 1.
(2) Chevrel, R.; Hirrien, M.; Sergent, M. *Polyhedron* **1986**, *5*, 87.
(3) Hughbanks, T.; Hoffmann, R. *J. Am. Chem. Soc.* **1983**, *105*, 1150.
(4) Prokopuk, N.; Kennedy, V. O.; Stern, C. L.; Shriver, D. F. *Inorg. Chem.* **1998**, *37*, 5001−5006.
(5) Maverick, A. W.; Gray, H. B. *J. Am. Chem. Soc.* **1981**, *103*, 1298.
(6) Copp, S. B.; Holman, K.; Subramanian, S.; Zaworotko, M. *J. Chem. Soc., Dalton Trans.* **1995**, 2233.
(7) Copp, S. B.; Subramanian, M. J.; Zaworotko, M. J. *Angew. Chem., Int. Ed. Engl.* **1993**, *32*, 706.
(8) Mironov, Y. V.; Virovets, A.; Naumev, N. G.; Ikorskii, V. N.; Fedorov, V. E. *Chem.*−*Eur. J.* **2000**, *6*, 1361.
(9) Prokopuk, N.; Weinert, C. S.; Siska, D. P.; Stern, C. L.; Shriver, D. F. *Angew. Chem., Int. Ed. Engl.* **2000**, *39*, 3312.
(10) Magliocchi, C.; Xie, X.; Hughbanks, T. *Inorg. Chem.* **2000**, *39*, 5000.
(11) Prokopuk, N.; Weinert, C. S.; Kennedy, V. O.; Siska, D. P.; Jeon, H. J.; Stern, C. L.; Shriver, D. F. *Inorg. Chim. Acta* **2000**, *300*−*302*, 951.
(12) Kennedy, V. O.; Stern, C. L.; Shriver, D. F. *Inorg. Chem.* **1994**, *33*, 5967.
(13) Johnston, D. H.; Stern, C. L.; Shriver, D. F. *Inorg. Chem.* **1993**, *32*, 5170.
(14) Johnston, D. H.; Gaswick, D. C.; Lonergan, M. C.; Stern, C. L.; Shriver, D. F. *Inorg. Chem.* **1992**, *31*, 1869.
(15) Weinert, C. S.; Stern, C. L.; Shriver, D. F. *Inorg. Chem.* **2000**, *39*, 240.
(16) Weinert, C. S.; Stern, C. L.; Shriver, D. F. *Inorg. Chim. Acta* **2000**, *307*, 139.
(17) Cotton, F. A.; Curtis, N. F. *Inorg. Chem.* **1965**, *4*, 241.
(18) Simsek, M. K.; Preetz, W. *Z. Anorg. Allg. Chem.* **1997**, *623*, 515.
(19) Preetz, W.; Bublitz, D.; Schnering, H. G. v.; Sassmannshausen, J. *Z. Anorg. Allg. Chem.* **1994**, *620*, 234.
(20) Bublitz, D.; Preetz, W.; Simsek, M. K. *Z. Anorg. Allg. Chem.* **1997**, *623*, 1.
(21) Preetz, W.; Harder, K.; Schnering, H. G. v.; Kliche, G.; Peters, K. *J. Alloys Compd.* **1992**, *183*, 413.
(22) Harder, K.; Peters, G.; Preetz, W. *Z. Anorg. Allg. Chem.* **1991**, *598/599*, 139.
(23) Bruckner, P.; Peters, G.; Preetz, W. *Z. Anorg. Allg. Chem.* **1993**, *619*, 551.
(24) Bruckner, P.; Peters, G.; Preetz, W. *Z. Anorg. Allg. Chem.* **1993**, *619*, 1920.
(25) Basic, I.; Brniceveic, N.; Beck, U.; Simon, A.; McCarley, R. E. *Z. Anorg. Allg. Chem.* **1998**, *624*, 725.
(26) Ehrlich, G. M.; Warren, C. J.; Haushalter, R. C.; DiSalvo, F. J. *Inorg. Chem.* **1995**, *34*, 4284.
(27) Johnston, D. H.; Shriver, D. F. *Inorg. Chem.* **1993**, *32*, 1045.
(28) Rao, K. M.; Prasad, R.; Agarwala, U. C. *Synth. React. Inorg. Met.-Org. Chem.* **1987**, *17*, 469.
(29) Robinson, L. M.; Bain, R. L.; Shriver, D. F.; Ellis, D. E. *Inorg. Chem.* **1995**, *34*, 5588.

10.1021/ic001480y CCC: $20.00

by the basicity of the incoming ligand, so clusters such as $[Bu_4N]_2[W_6Cl_8(O_2CCH_3)_6]$ and $[Bu_4N]_2[W_6Cl_8(N_3)_6]$ were unavailable from $[Bu_4N]_2[W_6Cl_8(OSO_2CF_3)_6]$.

A variety of polynuclear complexes containing the ambident cyanide group as a bridging ligand are known. These materials exhibit a variety of interesting properties, including electron transfer between remote sites,[30] multielectron transfer,[31,32] intervalent charge transfer,[19,33−35] and intramolecular energy transfer.[36−39] Prussian blue is a well-characterized example of such a complex. It consists of a three-dimensional cubic array of iron(III) centers coordinated to six $[Fe^{II}(CN)_6]^{4-}$ groups, and its intense blue color is attributed to light-induced charge transfer between the iron(II) and iron(III) centers.[28,40,41]

The basicity of the nitrogen end of cyanide is typically higher in electron-rich complexes.[28,42−45] This property has been employed to prepare cluster systems which contain organometallic complexes attached to a cluster framework through bridging cyanide ligands. For example, the complex $[(OC)Pd_4(\mu\text{-}NC)\text{-}Mn(C_5H_4CH_3)(CO)_2]_4$ was prepared from $[Pd_4(CO_4)(OC(O)\text{-}CH_3)_4][CH_3COOH]_2$ and $Na[(C_5H_5)Mn(CO)_2(CN)]$.[45] Also, the triflate ligands of $[Mo_6Cl_8(OSO_2CF_3)_2]^{2-}$ can be displaced by either $[(C_5H_5)Mn(CO)_2(CN)]^-$ or $(C_5H_5)Ru(PPh_3)_2(CN)$ to generate 12-metal clusters containing six organometallic complexes in the axial positions connected to the cluster core through cyanide bridges.[13]

In this paper we describe the synthesis and characterization of $[Bu_4N]_2[W_6Cl_8(p\text{-}OSO_2C_6H_4CH_3)_6]$ (**2**) and its use to extend the substitution chemistry developed using $[Bu_4N]_2[W_6Cl_8\text{-}(OSO_2CF_3)_6]$.

Experimental Section

IR spectra were obtained using a Bomem MB-100 Fourier transform infrared (FTIR) spectrometer with 2 cm^{-1} resolution on samples in solution, using CaF_2 solution cells with a 0.1 mm path length or as Nujol mulls sandwiched between KBr plates. UV/Visible (UV−vis) spectra were obtained using a Cary 1E UV/Vis spectrometer in 1.0 cm path length cells equipped to exclude air. ^1H and ^{13}C NMR spectra were recorded at 400 and 101 MHz, respectively, using a Varian Mercury-400 spectrometer. Elemental analyses were carried out by Midwest Microlabs. Mass spectra were obtained at the Analytical Services laboratory at Northwestern University.

Cyclic voltammograms were obtained with a Bioanalytical Systems 100B electrochemical analyzer. A platinum-disk working electrode and a platinum-foil counter electrode were employed in a single compartment cell. The reference electrode was a commercial (BAS) Ag/AgCl electrode, which was separated from the bulk solution by a porous Vycor tip. All electrochemical experiments were carried out at room temperature in dry N_2-purged cells with degassed solvents. The electrolyte $[Bu_4N][BF_4]$ was recrystallized from methanol/diethyl ether.

All manipulations were carried out under an atmosphere of nitrogen using a standard glovebox, a Schlenk line, and syringe techniques.[46] Solvents were dried using standard procedures and freshly distilled immediately before use. Reagents were purchased from Aldrich and used without further purification. The cluster $(H_3O)_2[W_6Cl_8Cl_6]\cdot 6H_2O$ was prepared by a literature route[47] and was converted to its tetrabutylammonium salt by metathesis with $[Bu_4N]Cl$. The bis(triphenylphosphine)iminium $[PPN]^+$, benzyltrimethylammonium $[BzMe_3N]^+$, and tetraphenylarsonium $[Ph_4As]^+$ salts of the cluster were prepared in an analogous manner. The complexes $[A][(C_5H_5)Mn(CO)_2(CN)]$ ($[A] = [Bu_4N]^+$, $[PPN]^+$, $[BzMe_3N]^+$, or $[Ph_4As]^+$),[48] $(C_5H_5)Ru\text{-}(PPh_3)_2(CN)$,[49] and $(C_5H_5)Os(PPh_3)_2(CN)$[49] were prepared by literature routes or slight variations thereof. The compound $[Bu_4N]_2[W_6Cl_8\text{-}(OSO_2CF_3)_6]$ (**1**) was prepared as previously described.[15]

Synthesis of $[Bu_4N]_2[W_6Cl_8(p\text{-}OSO_2C_6H_4CH_3)_6]$ (1). A Schlenk flask was charged with $[Bu_4N]_2[W_6Cl_8Cl_6]$ (0.419 g, 0.201 mmol) and $AgOSO_2C_6H_4CH_3$ (0.555 g, 2.00 mmol) in the glovebox. Dichloromethane (20 mL) was added, and the suspension was stirred in the absence of light for 5 h and then filtered through Celite. The yellow filtrate was concentrated to 5 mL, and diethyl ether was added dropwise (15 mL), resulting in a yellow precipitate, which was isolated by vacuum filtration, washed with Et_2O (3 × 5 mL), and dried in vacuo to yield 0.475 g (82%) of **1**. Anal. Calcd for $C_{74}H_{114}Cl_8O_{18}N_2S_6W_6$: C, 30.66; H, 3.96; N, 0.97. Found: C, 30.64; H, 4.00; N, 0.93. ^1H NMR (CD_2Cl_2): 2.38 (s, 18H, H_3C), 7.22 (d, 12 H, H *ortho* to CH_3), 7.63 (d, 12 H, H *ortho* to SO_3) ppm. ^{13}C NMR (CD_2Cl_2): 21.8 (CH_3), 126.7 (C *ortho* to CH_3), 129.5 (C *ortho* to SO_3), 139.9 (*ipso*-C−CH_3), 142.0 (*ipso*-C−SO_3).

Synthesis of $[Bu_4N]_2[W_6Cl_8(NCO)_6]$ (2). A solution of NaNCO (0.027 g, 0.415 mmol) in 2 mL of methanol was added to a Schlenk flask charged with **1** (0.180 g, 0.0621 mmol) and 2 mL of ethanol. This NaNCO solution was added to the cluster, resulting in the formation of a precipitate, which was isolated by filtration and washed with 3 × 5 mL of methanol. The solid was dissolved in 2 mL of CH_2Cl_2, the solution was filtered, and 5 mL of diethyl ether was added dropwise to the filtrate, resulting in the formation of a yellow precipitate, which was isolated by filtration, washed with 3 × 3 mL of diethyl ether, and dried in vacuo to yield 0.073 g (56%) of **2**. Anal. Calcd for $C_{32}H_{72}\text{-}Cl_8N_8O_6W_6$: C, 21.49; H, 3.42; N, 5.28. Found: C, 21.42; H, 3.48; N, 5.23.

Synthesis of $[Bu_4N]_2[W_6Cl_8(NCS)_6]$ (3) and $[Bu_4N]_2[W_6Cl_8\text{-}(NCSe)_6]$ (4). A solution of KNCS (0.033 g, 0.340 mmol) in 2 mL of methanol was prepared. A Schlenk flask was charged with **1** that was dissolved in 2 mL of methanol. The KNCS solution was added, resulting in the formation of a brown precipitate. The solution was filtered immediately to remove MeOH, the resulting residue was dissolved in 6 mL of CH_2Cl_2 and filtered, and the volume was reduced to approximately 2 mL. Diethyl ether (5 mL) was added dropwise, resulting in a yellow precipitate, which was isolated by filtration, washed with 3 × 2 mL of Et_2O, and dried in vacuo to yield 0.052 g (56%) of **3**. Cluster **4** was prepared by an analogous procedure using KNCSe (0.045 g, 0.312 mmol) and **1** (0.103 g, 0.0355 mmol). Yield: 0.047 g (53%). Anal. Calcd for $C_{38}H_{72}Cl_8N_8S_6W_6$: C, 20.56; H, 3.27; N, 5.05. Found: C, 20.54; H, 3.31; N, 5.08. Anal. Calcd for $C_{38}H_{72}Cl_8N_8\text{-}Se_6W_6$: C, 18.24; H, 2.90; N, 4.48. Found: C, 18.11; H, 2.80; N, 4.43.

Synthesis of $[Bu_4N]_2[W_6Cl_8(O_2CCH_3)_6]$ (5). A solution of sodium acetate (0.035 g, 0.257 mmol) in 1 mL of methanol was prepared. A Schlenk flask was charged with 0.080 g (0.0276 mmol) of **1** and 0.5 mL of methanol. The NaOAc solution was added to the cluster solution

---

(30) Vogler, A.; Kunkley, H. *Inorg. Chim. Acta* **1988**, *150*, 1.
(31) Zhou, M.; Pfennig, B. W.; Steiger, J.; Van Engen, D.; Bocarsly, A. B. *Inorg. Chem.* **1990**, *29*, 2456.
(32) Pfennig, B. W.; Bocarsly, A. B. *Coord. Chem. Rev.* **1991**, *111*, 91.
(33) Bignozzi, C. A.; Roffia, S.; Chiorboli, C.; Davila, J.; Indelli, M. T.; Scandola, F. *Inorg. Chem.* **1989**, *28*, 4350.
(34) Bignozzi, C. A.; Argazzi, R.; Schoonover, J. R.; Gordon, K. C.; Dyer, R. B.; Scandola, F. *Inorg. Chem.* **1992**, *31*, 5260.
(35) Dong, Y.; Hupp, J. T. *Inorg. Chem.* **1992**, *31*, 3322.
(36) Bignozzi, C. A.; Indelli, M. T.; Scandola, F. *J. Am. Chem. Soc.* **1989**, *111*, 5192.
(37) Bignozzi, C. A.; Roffia, S.; Scandola, F. *J. Am. Chem. Soc.* **1985**, *107*, 1644.
(38) Bignozzi, C. A.; Paradisi, C.; Roffia, S.; Scandola, F. *Inorg. Chem.* **1988**, *327*, 408.
(39) Kalyanasundaram, K.; Gratzel, M.; Nazeeruddin, M. K. *Inorg. Chem.* **1992**, *31*, 5243.
(40) Creutz, C. *Prog. Inorg. Chem.* **1983**, *30*, 1.
(41) Hush, N. S. *Prog. Inorg. Chem.* **1967**, *8*, 391.
(42) Prasad, R.; Mishra, L.; Agarwala, U. C. *Indian J. Chem.* **1991**, *30A*, 45.
(43) Oswald, B.; Powel, A. K.; Rashwan, F.; Heinze, J.; Vahrenkamp, H. *Chem. Ber.* **1990**, *123*, 243.
(44) Deeming, A. J.; Proud, G. P.; Dawes, H. M.; Hursthouse, M. B. *J. Chem. Soc., Dalton Trans.* **1988**, 2475.
(45) Braunstein, P.; Oswald, B.; Tiripicchio, A.; Camellini, M. T. *Angew. Chem., Int. Ed. Engl.* **1990**, *29*, 1140.
(46) Shriver, D. F.; Drezdzon, M. A. *The Manipulation of Air-Sensitive Compounds*, 2nd ed.; John Wiley & Sons: New York, 1986.
(47) Dorman, W. C.; McCarley, R. E. *Inorg. Chem.* **1974**, *13*, 491.
(48) Fischer, E. O.; Schneider, R. J. J. *J. Organomet. Chem.* **1968**, *12*, 27.
(49) Baird, G. J.; Davies, S. G. *J. Organomet. Chem.* **1984**, *262*, 215.

via syringe, and the reaction mixture was stirred for 3 min, followed by the removal of CH_3OH under vacuum. Dichloromethane (2 mL) was then added to the yellow/brown solid, the resulting solution was filtered, and the insoluble material was washed with 2 × 1 mL of CH_2Cl_2. The filtrate was layered with diethyl ether (5 mL), resulting in the formation of a light brown oil. The CH_2Cl_2/Et_2O mixture was decanted from the oil, and 3 mL of Et_2O was added. The flask was swirled, and the ether was decanted. This process was repeated three times, resulting in a yellow solid, which was isolated by filtration, washed with diethyl ether (3 × 2 mL), and dried in vacuo to yield 0.028 g (46%) of **5**. Anal. Calcd for $C_{44}H_{90}Cl_8N_2O_{12}W_6$: C, 23.74; H, 4.08; N, 1.26. Found: C, 24.05; H, 4.17; N, 1.33. ^1H NMR (CD_2Cl_2): 2.00 ppm (s, $-OC(O)CH_3$).

Synthesis of $[Bu_4N]_2[W_6Cl_8\{(\mu\text{-}NC)Mn(CO)_2(C_5H_5)\}_6]$ (6). A Schlenk flask was charged with **1** (0.068 g, 0.0234 mmol) and $[Bu_4N][(C_5H_5)Mn(CO)_2(CN)]$ (0.081 g, 0.182 mmol). Dichloromethane was added (5 mL), and the red/brown solution was stirred for 2 h. Concentration of the solution to approximately 2 mL, followed by careful addition of diethyl ether, resulted in the formation of a red/brown precipitate, which was isolated by filtration, washed with 3 × 3 mL of diethyl ether, and dried in vacuo to yield 0.042 g (58%) of product. Anal. Calcd for $C_{80}H_{102}Cl_8Mn_6N_8O_{12}W_6$: C, 31.16; H, 3.33; N, 3.63. Found: C, 31.85; H, 3.58; N, 3.82.

Synthesis of $[W_6Cl_8\{(\mu\text{-}NC)Ru(PPh_3)_2(C_5H_5)\}_6][p\text{-}OSO_2C_6H_4CH_3]_4$ (7). To a Schlenk flask charged with **2** (0.102 g, 0.0369 mmol) and $(C_5H_5)Ru(PPh_3)_2(CN)$ (0.163 g, 0.227 mmol), 10 mL of dichloromethane was added. The solution was stirred for 3 h and concentrated to 3 mL, and diethyl ether (8 mL) was added dropwise, resulting in a yellow precipitate, which was isolated by filtration, washed with diethyl ether (3 × 5 mL), and dried in vacuo to yield 0.168 g (73%) of product. Anal. Calcd for $C_{280}H_{238}Cl_8N_6O_{12}P_{12}Ru_6S_4W_6$: C, 52.78; H, 3.76; N, 1.32. Found: C, 51.27; H, 3.43; N, 1.17.

Synthesis of $[W_6Cl_8\{(\mu\text{-}NC)Os(PPh_3)_2(C_5H_5)\}_6][p\text{-}OSO_2C_6H_4CH_3]_4$ (8). A Schlenk flask was charged with **1** (0.164 g, 0.0592 mmol) and $(C_5H_5)Os(PPh_3)_2(CN)$ (0.289 g, 0.358 mmol). Dichloromethane was added (8 mL), and the solution was stirred for 3 h. The solution was concentrated in volume to approximately 3 mL, and diethyl ether (7 mL) was added dropwise, resulting in a yellow/red precipitate, which was isolated by filtration, washed with diethyl ether (3 × 5 mL), and dried in vacuo to yield 0.345 g (86%) of product. Anal. Calcd for $C_{280}H_{238}Cl_8N_6O_{12}Os_6P_{12}S_4W_6$: C, 48.69; H, 3.47; N, 1.22. Found: C, 48.08; H, 3.28; N, 1.17.

Crystal Structures of $[Bu_4N]_2[W_6Cl_8(p\text{-}OSO_2C_6H_4CH_3)_6]$ (1), $[Bu_4N]_2[W_6Cl_8(NCSe)_6]\cdot Et_2O\cdot{}^1/_2CH_2Cl_2$ (4), and $[Bu_4N]_2[W_6Cl_8(O_2CCH_3)_6]$ (5). Yellow crystals of **1**, **4**, and **5** were grown by slow diffusion of diethyl ether into a CH_2Cl_2 solution of the cluster. Crystals measuring 0.25 × 0.20 × 0.34 mm for **1**, 0.03 × 0.15 × 0.04 mm for **4**, or 0.11 × 0.07 × 0.27 mm for **5** were mounted on individual glass fibers using Paratone-N oil (Exxon) and transferred to the N_2 cold stream (−120 °C) of a Bruker CCD diffractometer. All measurements were made with graphite-monochromated Mo Kα radiation. A set of 25 carefully centered reflections was used to determine the cell constants. On the basis of the systematic absences of $0kl$ ($k \pm 2n$), $h0l$ ($l \pm 2n$), and $hk0$ ($h \pm 2n$) the space group was determined to be *Pbca* (# 61) for **1**. Similarly, on the basis of the systematic absences of $h0l$ ($h + l \pm 2n$) and $0k0$ ($k \pm 2n$) the space group was determined to be $P2_1/n$ (#14) for both **4** and **5**. Data were collected at −120 °C to a maximum 2θ value of 56.6°. For **1** and **5**, data were collected in 0.30° oscillations with 15.0 s exposure times, while for **4** the exposure time was 25.0 s. The crystal-to-detector distance was 50.00 mm, and the detector swing angle was 28.00° in all cases. For **1**, a total of 91 185 reflections were collected of which 13 082 were unique ($R_{int} = 0.053$). The data were corrected for Lorentz and polarization effects for **1**, **4**, and **5**. For **1**, a Gaussian face-indexed absorption correction was used and a correction for secondary extinction was applied (coefficient = $3.675e^{-9}$). Minimum and maximum transmission factors were 0.14 and 0.28, respectively. For **4**, of the 34 036 reflections which were collected 9144 were unique ($R_{int} = 0.121$). An integration absorption correction was applied. Minimum and maximum transmission factors were 0.2847 and 0.696 8, respectively. For **5**, a total of 29 822 reflections were collected of which 7995 were unique ($R_{int} = 0.056$). An analytical face-indexed absorption correction was applied. Minimum and maximum transmission factors were 0.12 and 0.49, respectively.

Table 1. IR Data for $[Bu_4N]_2[W_6Cl_8(p\text{-}OSO_2C_6H_4CH_3)_6]$ (**1**), $[Bu_4N]_2[W_6Cl_8(OSO_2CF_3)_6]$ (**9**), and $AgOSO_2C_6H_4CH_3$ in Nujol Mull

species	ν_{as} (SO_3), cm^{-1}	ν_s (SO_3), cm^{-1}
$AgOSO_2C_6H_4CH_3$	1194	1152
$[Bu_4N]_2[W_6Cl_8(p\text{-}OSO_2C_6H_4CH_3)_6]$ (**1**)	1282	953
	1158	
$[Bu_4N]_2[W_6Cl_8(OSO_2CF_3)_6]$ (**9**)	1346	997
	1196	

In all cases, all calculations were carried out using the teXsan crystallographic software package (Molecular Structure Corp.).[50] The structure was solved using direct methods[51] and expanded using Fourier techniques. Neutral atom scattering factors were taken from Cromer and Waber.[52] Anomalous dispersion effects were included in F_{calc}.[53] The values of $\Delta f'$ and $\Delta f''$were those of Creagh and Hubbell.[54] The values for the mass attenuation coefficients were those of Creagh and McAuley.[55]

For **1** and **5**, the non-hydrogen atoms were refined anisotropically and the hydrogen atoms were included in idealized positions but not refined. Owing to a paucity of data for **4**, the tungsten atom, only the selenium atoms, and the cluster anion chlorine atoms were refined anisotropically, while the rest were refined isotropically. Hydrogen atoms were included in idealized positions (except for on the disordered carbon atoms on the cation and the solvent molecules) but not refined. For **1**, the final cycle of full matrix least-squares refinement on F^2, based on 8803 observed reflections and 542 variable parameters, converged to an R value of 0.025 ($R_w = 0.053$). The standard deviation of a unit weight was 1.36. For **4**, the refinement was based on 2484 observed reflections and 211 variable parameters and converged (largest parameter shift was 0.00 times its esd) to an R value of 0.044 ($R_w = 0.088$). The standard deviation of a unit weight was 1.36. For **5**, 5601 observed reflections and 325 variable parameters were employed and the structure refinement converged to an R value of 0.046 ($R_w = 0.061$), with a 1.33 standard deviation of a unit weight.

In all cases, the weighting scheme was based on counting statistics. Plots of $\sum w(|F_o| - |F_c|)^2$ vs $|F_o|$, reflection order in data collection, $\sin \theta/\lambda$, and various classes of indices showed no unusual trends. The maximum and minimum peaks on the final difference Fourier map corresponded to 2.07 and -1.27 e$^-$/Å^3 (**1**), 2.11 and -1.31 e$^-$/ Å^3 (**4**), and 2.52 and -1.39 e$^-$/Å^3 (**5**), respectively, and were located in the vicinity of the tungsten positions in all cases.

Results and Discussion

The tosylate cluster **1** can be prepared from $[Bu_4N]_2[W_6Cl_8Cl_6]$ and silver tosylate in excellent yield. IR data for **1** and $AgOSO_2C_6H_5CH_3$ is summarized in Table 1. Assignments of the SO_3-stretching bands is based on comparison with those of $[Bu_4N]_2[W_6Cl_8(OSO_2CF_3)_6]$ (**9**),[15] $[Bu_4N]_2[Mo_6Cl_8(OSO_2CF_3)_6]$,[14] $[Bu_4N]_2[Mo_6Cl_8(OSO_2C_6H_4CH_3)_6]$,[56] and several mononuclear complexes containing tosylate ligands bound

---

(50) *Texsan, Crystal Structure Analysis Package*; Molecular Structure Corporation: The Woodlands, TX, 1985 and 1992.

(51) Sheldrick, G. M. SHELXS86. In *Crystallographic Computing3*; Sheldrick, G. M., Kruger, C., Goddard, R., Eds.; Oxford University Press: Oxford, 1985; pp 175−189.

(52) Cromer, D. T.; Waber, J. T. *International Tables for X-ray Crystallography*; The Kynoch Press: Birmingham, England, 1974; Vol. IV.

(53) Ibers, J. A.; Hamilton, W. C. *Acta Crystallogr.* **1964**, *17*, 781.

(54) Creagh, D. C.; Hubbell, J. H. *International Tables for X-ray Crystallography*; Kluwer Academic Publishers: Boston, 1992; Vol. C, Table 2.3.4.3, pp 200−206.

(55) Creagh, D. C.; McAuley, W. J. *International Tables for X-ray Crystallography*; Kluwer Academic Publishers: Boston, 1992; Vol. C.

(56) Johnston, D. H. Ph.D. Thesis, Northwestern University, Evanston, IL, 1993.

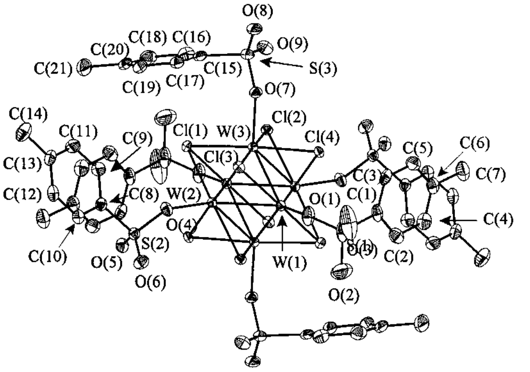

Figure 1. ORTEP diagram of the cluster anion of $[Bu_4N]_2[W_6Cl_8(OSO_2C_6H_4CH_3)_6]\cdot 2CH_2Cl_2$ (**1**). Thermal ellipsoids are drawn at 50% probability.

Table 2. Crystallographic Data for $[Bu_4N]_2[W_6Cl_8(OSO_2C_6H_4CH_3)_6]\cdot 2\ CH_2Cl_2$ ($\mathbf{1}\cdot 2CH_2Cl_2$), $[Bu_4N]_2[W_6Cl_8(NCSe)_6]\cdot Et_2O\cdot {}^1/_2CH_2Cl_2$ ($\mathbf{4}\cdot Et_2O\cdot {}^1/_2CH_2Cl_2$), and $[Bu_4N]_2[W_6Cl_8((OC(O)CH_3)_6]$ (**5**)

emp. formula	$C_{76}H_{118}C_{12}$-$O_{18}N_2S_6W_6$	$C_{42.5}H_{67}Cl_9$-$N_8OSe_6W_6$	$C_{44}H_{90}Cl_8$-$N_2O_{12}W_6$
formula wt.	3068.67	2601.99	2225.93
space group	*Pbca* (# 61)	$P2_1/n$ (# 14)	$P2_1/n$ (# 14)
a, Å	24.5320(6)	11.2034(9)	10.4369(1)
b, Å	15.8886(5)	16.471(1)	14.182(2)
c, Å	25.3159(4)	20.038(2)	21.891(3)
β, deg		95.256(2)	94.220(2)
V, Å^3	9867.61(5)	3680.0(5)	3231.5(6)
Z	4	2	2
ρ_{calcd}, g cm^{-3}	2.065	2.348	2.287
μ, cm^{-1} (Mo Kα)	74.87	126.79	110.30
rad. (Mo Kα) (Å)	$\lambda = 0.710\ 69$	$\lambda = 0.710\ 69$	$\lambda = 0.710\ 69$
T, °C	−120	−120	−120
$R(F)^a$	0.025	0.044	0.046
$R_w(F)^b$	0.053	0.088	0.061

[a] $R(F) = [\Sigma|(|F_o| - |F_c|)|/\Sigma|F_o|]$. [b] $R_w(F) = [\Sigma w(|F_o| - |F_c|)^2/\Sigma|F_o|^2]^{1/2}$ and $w = 4F_o2/\sigma^2(F_o2)$.

Table 3. Selected Bond Distances (Å) and Angles (deg) for $[Bu_4N]_2[W_6Cl_8(OSO_2C_6H_4CH_3)_6]\cdot \mathbf{2}CH_2Cl_2$ ($\mathbf{1}\cdot 2CH_2Cl_2$)

W(1)−O(1)	2.094(3)	W(2)−O(4)	2.086(3)
W(3)−O(7)	2.099(3)	S(1)−O(1)	1.479(4)
S(1)−O(2)	1.486(5)	S(1)−O(3)	1.381(5)
S(1)−C(1)	1.764(6)	S(2)−O(4)	1.504(4)
S(2)−O(5)	1.442(3)	S(2)−O(6)	1.439(4)
S(2)−C(8)	1.766(5)	S(3)−O(7)	1.517(3)
S(3)−O(8)	1.443(4)	S(3)−O(9)	1.432(4)
S(3)−C(15)	1.764(5)		
W(1)−O(1)−S(1)	141.9(2)	W(2)−O(4)−S(2)	138.5(2)
W(3)−O(7)-S(3)	137.4(2)		

to a metal center.[57−61] The tosylate ligand is similar to the triflate ligand in that the symmetry is lowered from C_{3v} to C_s upon coordination to the cluster. This results in the splitting of the degenerate $\nu_{as}(SO_3)$ band in the free ligand at 1194 cm^{-1} into two bands at 1282 and 1158 cm^{-1}. The $\nu_s(SO_3)$ stretch at 953 cm^{-1} is significantly lower in energy relative to that of $AgOSO_2C_6H_4CH_3$ at 1152 cm^{-1}. A similar effect was observed for the $\nu_s(SO_3)$ band of the triflate clusters **9** and $[Bu_4N]_2[Mo_6Cl_8(OSO_2CF_3)_6]$.[14,15]

An X-ray crystal structure of **1** was obtained, the ORTEP plot of the cluster anion is shown in Figure 1, crystallographic data are summarized in Table 2, and selected bond lengths and angles are summarized in Table 3. The structure of the $\{W_6Cl_8\}^{4+}$ core is similar to previously characterized tungsten clusters.[1,15,16,62−66] The average W−O distance is 2.093 Å and the average W−O−S bond angle is 139.3°, which are typical values for tosylate groups bound to metal centers through one oxygen atom.[60,61,67−69] The benzene rings are nearly planar and exhibit bond lengths and angles that closely resemble those of the free ion.[70,71] The S═O bond lengths for the uncoordinated oxygen atoms are similar to the S═O bond lengths in the free ion, with an average value of 1.437 Å. The S−O bond for the coordinated oxygen is elongated compared to those of the free ligand, with an average length of 1.500 Å. The environment about the sulfur atoms approaches tetrahedral in all cases.

Cluster **1** is more stable in alcoholic solvents than the triflate cluster **9**. While **9** becomes an intractable brown oil within 3−4 min in methanol, **1** is stable for up to 10 min. This difference appears to originate from the tosylate anion functioning as a stronger donor to the tungsten atoms relative to the triflate anion. The pK_b of the tosylate ion is approximately 20, while that of the triflate ion is about 29.[72−74] In this connection, clusters with strongly donating ligands (chloride, thiocyanate, etc.) are stable in methanol.

The greater stability of **1** in methanol allows the preparation of the pseudohalide clusters **2**−**4** to result in higher yields in comparison to the triflate cluster **9**. Yields are typically 15−20% greater when **1** is used as the starting material instead of **9**. When starting with **1**, analytically pure material was obtained for clusters **2**−**4** without recrystallization and X-ray quality crystals of **4** were easily grown. An ORTEP plot for the cluster anion of **4** is shown in Figure 2, crystallographic data are summarized in Table 2, and selected bond lengths and angles are listed in Table 4. The spectroscopic characterization of **4** has been previously reported.[15] The selenocyanate ligands are bound to the cluster in a manner analogous to those of $[Bu_4N]_2[Mo_6Br_8(NCSe)_6]$.[18] The cluster core bond lengths and angles of **4** are again typical for species containing the $\{W_6Cl_8\}^{4+}$ unit.[1,15,16,62−66] The W−N−C bond angles have an average value of 167.7°, which is considerably larger than that of the thiocyanate ligands in $[Bu_4N]_2[W_6Cl_8(NCS)_6]$.[15,63] The selenocyanate ligands are nearly linear, with an average N−C−Se bond angle of 177.3°. The average carbon-to-nitrogen distance of 1.06 Å indicates the presence of a C−N triple bond, as expected, and the average C−Se bond distance is 1.86 Å.

---

(57) Manhas, B. S.; Bhatia, V. K. *J. Inorg. Nucl. Chem.* **1975**, *37*, 1799.
(58) Kapila, V. P.; Kapila, B.; Kumar, S. *Indian J. Chem.* **1991**, *30A*, 908.
(59) Ruther, R.; Huber, F.; Preut, H. *J. Organomet. Chem.* **1988**, *342*, 185.
(60) Coe, B. J.; McDonald, C. I.; Beddoes, R. L. *Polyhedron* **1998**, *17*, 1997.
(61) Bailey, O. H.; Ludi, A. *Inorg. Chem.* **1985**, *24*, 2582.
(62) Zietlow, T. C.; Schaefer, W. P.; Sadeghi, B.; Hua, N.; Gray, H. B. *Inorg. Chem.* **1986**, *25*, 2195.
(63) Stallmann, M.; Preetz, W. *Z. Anorg. Allg. Chem.* **1999**, *625*, 567.
(64) Stallmann, M.; Preetz, W. *Z. Anorg. Allg. Chem.* **2000**, *626*, 258.
(65) Ihmaine, S.; Perrin, C.; Sergent, M. *Eur. J. Solid State Inorg. Chem.* **1997**, *34*, 169.
(66) Healy, P. C.; Kepert, D. L.; Taylor, D.; White, A. H. *J. Chem. Soc., Dalton Trans.* **1973**, 646.
(67) Harding, F. A.; Preece, M.; Robinson, S. D.; Henrick, K. *Inorg. Chim. Acta* **1986**, *118*, L31.
(68) Harding, P. A.; Robinson, S. D.; Henrick, K. *J. Chem. Soc., Dalton Trans.* **1988**, 415.
(69) Kolle, U.; Gorissen, R.; Wagner, T. *Chem. Ber.* **1995**, *128*, 911.
(70) Rogers, R. D.; Bond, A. H.; Henry, R. F. *Acta Crystallogr., Sect. C* **1991**, *C47*, 168.
(71) Arora, S. K.; Sundaralingam, M. *Acta Crystallogr., Sect. B* **1971**, *B27*, 1293.
(72) Greenwood, N. N.; Earnshaw, A. *Chemistry of the Elements*; Pergamon Press: Oxford, 1984.
(73) March, J. *Advanced Organic Chemistry*, 4th ed.; John Wiley and Sons: New York, 1992.
(74) Cotton, F. A.; Wilkinson, G. *Advanced Inorganic Chemistry*, 5th ed.; John Wiley and Sons: New York, 1988.

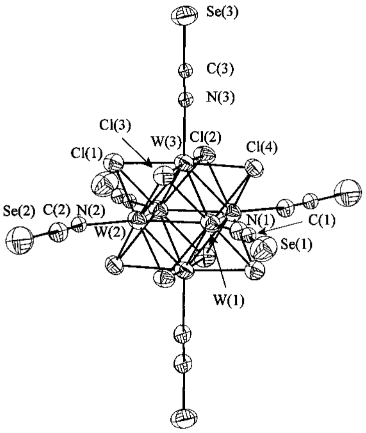

Figure 2. ORTEP plot of the cluster anion of $[Bu_4N]_2[W_6Cl_8(NCSe)_6]\cdot Et_2O\cdot{}^1/_2CH_2Cl_2$ (**4**). Thermal ellipsoids are drawn at 50% probability.

Table 4. Selected Bond Lengths (Å) and Angles (deg) for $[Bu_4N]_2[W_6Cl_8(NCSe)_6]\cdot Et_2O\cdot{}^1/_2CH_2Cl_2$ ($\mathbf{4}\cdot Et_2O\cdot{}^1/_2CH_2Cl_2$)

W(1)−N(1)	2.07(2)	W(2)−N(2)	2.12(2)
W(3)−N(3)	2.11(2)	N(1)−C(1)	1.08(2)
N(2)−C(2)	1.06(2)	N(3)−C(3)	1.03(3)
C(1)−Se(1)	1.88(3)	C(2)−Se(2)	1.82(3)
C(3)−Se(3)	1.89(3)		
W(1)−N(1)−C(1)	168.2(2)	W(2)−N(2)−C(2)	167.4(2)
W(3)−N(3)−C(3)	173.5(2)	N(1)−C(1)−Se(1)	176.7(2)
N(2)−C(2)−Se(2)	178.7(2)	N(3)−C(3)−Se(3)	176.6(2)

Table 5. IR Data for NaO_2CCH_3 and the Acetate Clusters $[Bu_4N]_2[M_6Cl_8((OC(O)CH_3)_6]$ (M = Mo, W)

species	IR bands (cm^{-1})	assignmt	ref
NaO_2CCH_3	1576	ν(C═O)	75
$[Bu_4N]_2[Mo_6Cl_8(OC(O)CH_3)_6]$	1339	ν(C−O)	75
$[Bu_4N]_2[W_6Cl_8(OC(O)CH_3)_6]$ (**5**)	1704	ν(C═O)	56
	1403	ν(C−O)	56
	1636	ν(C═O)	*a*
	1361	ν(C−O)	*a*

[a] This paper.

These average distances and angles are similar to those found in $[Bu_4N]_2[Mo_6Br_8(NCSe)_6]$.[18]

Cluster **1** also appears to be more resistant to decomposition than the triflate cluster **9** in the presence of basic ligands. Attempts to prepare **5** from **9** using tetrabutylammonium acetate in CH_2Cl_2 or sodium acetate in MeOH resulted in decomposition.[15] However, **5** is available from **1** and sodium acetate in modest yield. An oil is initially obtained in the preparation of **5**, but extraction with diethyl ether results in the formation of a solid yellow product. Attempts to prepare **5** from $Ag(O_2CCH_3)$ and $[Bu_4N]_2[W_6Cl_8Cl_6]$ were unsuccessful.

Cluster **5** was characterized by NMR and IR spectroscopy and an X-ray crystal structure determination. The ^1H NMR spectrum of **5** contains a resonance at 2.00 ppm for the hydrogen atoms of the acetate ligands. IR data for **5**, $[Bu_4N]_2[Mo_6Cl_8(O_2CCH_3)_6]$,[56] and $Na(O_2CCH_3)$[75] are summarized in Table 5. The IR bands of **5** at 1639 and 1365 cm^{-1} are assigned to the ν(C═O) and ν(C−O) modes, respectively. These bands are shifted from those of sodium acetate, which appear at 1576 (ν(C═O)) and 1339 (ν(C−O)) cm^{-1}.[75]

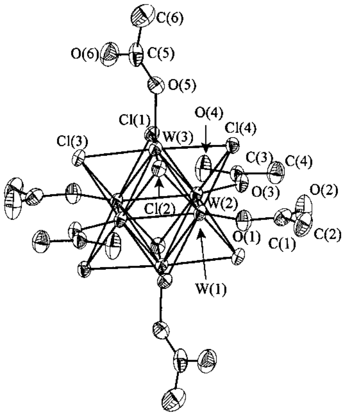

Figure 3. ORTEP diagram of the cluster anion of $[Bu_4N]_2[W_6Cl_8(OC(O)CH_3)_6]$ (**5**). Thermal ellipsoids are drawn at 50% probability.

Table 6. Selected Bond Lengths (Å) and Angles (deg) for $[Bu_4N]_2[W_6Cl_8(O_2CCH_3)_6]$ (**5**)

W(1)−O(1)	2.106(5)	W(2)−O(3)	2.086(5)
W(3)−O(5)	2.098(5)	O(1)−C(1)	1.272(8)
O(3)−C(3)	1.274(8)	O(5)−C(5)	1.270(9)
C(1)−O(2)	1.224(9)	C(3)−O(4)	1.232(8)
C(5)−O(6)	1.241(9)	C(1)−C(2)	1.522(1)
C(3)−C(4)	1.507(1)	C(5)−C(6)	1.534(1)
W(1)−O(1)−C(1)	130.0(5)	W(2)−O(3)−C(3)	127.8(4)
W(3)−O(5)−C(5)	131.3(5)	O(1)−C(1)−O(2)	125.7(7)
O(1)−C(1)−C(2)	113.6(7)	O(2)−C(1)−C(2)	120.6(7)
O(3)−C(3)−O(4)	124.4(7)	O(3)−C(3)−C(4)	115.6(6)
O(4)−C(3)−C(4)	119.9(7)	O(5)−C(5)−O(6)	127.3(8)
O(5)−C(5)−C(6)	115.4(7)	O(6)−C(5)−C(6)	117.3(8)

An ORTEP plot for the cluster anion of **5** is shown in Figure 3, crystallographic data are summarized in Table 2, and selected bond lengths and angles are listed in Table 6. The structure of the cluster core is again typical for systems containing the $\{W_6Cl_8\}^{4+}$ fragment.[1,15,16,62−66] The average W−O bond length is 2.097 Å and the average W−O−C bond angle is 129.7°, which are typical for complexes containing a monodentate acetate ligand.[76−78] The C−O distances range from 1.270 to 1.274 Å for the coordinated oxygen atoms (average value = 1.272 Å), while the C═O distances range from 1.224 to 1.241 Å (average value = 1.232 Å) for the carbonyl moieties of the ligands. The O−C═O angles have an average value of 125.8°, which is slightly larger than the expected value, while the $O-C_{carbonyl}-C_{methyl}$ angles are slightly narrower, with an average value of 116.1°.

Although **5** is available from **1**, attempts to prepare the azide cluster $[Bu_4N]_2[W_6Cl_8(N_3)_6]$ or the cyanide cluster $[Bu_4N]_2[W_6Cl_8(CN)_6]$ were unsuccessful. Reaction of **1** with sodium azide in methanol yielded a yellow solid product instead of the oil found for **9**. The IR spectrum of the product showed bands at 2044 (ν_{as}(NNN)), 1323 (ν_s(NNN)), and 642 cm^{-1} (δ(NNN)), which are characteristic of bound azide ligands in related clusters.[20] However, analytically pure material could not be obtained. Reaction of **1** with sodium cyanide, sodium methoxide, or other strongly basic ligands resulted in intractable products, which lacked diagnostic bands in their IR spectra.

Three clusters containing six axial organometallic ligands, **6**, **7**, and **8**, were prepared from **1**. Although spectroscopic data and elemental analysis confirm the successful syntheses of the clusters **6**−**8**, crystals of sufficient quality for an X-ray structure

---

(75) Baillie, M. J.; Brown, D. H.; Moss, K. C.; Sharp, D. W. A. *J. Chem. Soc. A* **1968**, 3110.

(76) Cotton, F. A.; Darensbourg, D. J.; Kolthammer, B. W. S.; Kudaroski, R. *Inorg. Chem.* **1982**, *21*, 1656.

(77) Fairhurst, S. A.; Henderson, R. A.; Hughes, D. L.; Ibrahim, S. K.; Pickett, C. J. *J. Chem. Soc., Chem. Commun.* **1995**, 1569.

(78) Werner, H.; Roll, J.; Zolk, R.; Thometzek, P.; Linse, K.; Ziegler, M. L. *Chem. Ber.* **1987**, *120*, 1553.

Table 7. Electrospray (ES^-) Mass Spectral Data for $[Bu_4N]_2[W_6Cl_8\{(\mu\text{-}NC)Mn(CO)_2(C_5H_5)\}_6]$ (**6**)

species	mass (highest intensity) calcd	mass (highest intensity) obs	rel intensity	*R* (%)
$[W_6Cl_8\{(\mu\text{-}NC)Mn(CO)_2(C_5H_5)\}_6]^{2-}$	1300	1300	63.8	3.18
$[W_6Cl_8(NC)\{(\mu\text{-}NC)Mn(CO)_2(C_5H_5)\}_5]^{2-}$	1212	1213	100	4.22
$[W_6Cl_8(NC)_2\{(\mu\text{-}NC)Mn(CO)_2(C_5H_5)\}_4]^{2-}$	1124	1124	84.3	3.52
$[W_6Cl_8(NC)_3\{(\mu\text{-}NC)Mn(CO)_2(C_5H_5)\}_3]^{2-}$	1036	1038	32.4	4.89
$[W_6Cl_8(NC)_4\{(\mu\text{-}NC)Mn(CO)_2(C_5H_5)\}_2]^{2-}$	948	950	8.3	5.67
$[W_6Cl_8(NC)_5\{(\mu\text{-}NC)Mn(CO)_2(C_5H_5)\}]^{2-}$	860	860	3.8	6.53

Table 8. IR Data for Clusters **6**−**8**, **10**, and the Corresponding Free Complexes

complex	ν_{CO}, cm^{-1}	ν_{CN}, cm^{-1}
$[Bu_4N][(C_5H_5)Mn(CO)_2(CN)]$[a]	1906, 1831	2060
$[Bu_4N]_2[W_6Cl_8\{(\mu\text{-}NC)Mn(CO)_2(C_5H_5)\}_6]$ (**7**)	1918, 1865	2030
$[Bu_4N]_2[Mo_6Cl_8\{(\mu\text{-}NC)Mn(CO)_2(C_5H_5)\}_6]$ (**10**)[b]	1916, 1866	2028
$(C_5H_5)Ru(PPh_3)_2(CN)$[c]		2072
$[W_6Cl_8\{(\mu\text{-}NC)Ru(PPh_3)_2(C_5H_5)\}_6][OSO_2CF_3]_4$ (**8**)		2009
$(C_5H_5)Os(PPh_3)_2(CN)$[c]		2067
$W_6Cl_8\{(\mu\text{-}NC)Os(PPh_3)_2(C_5H_5)\}_6][OSO_2CF_3]_4$ (**9**)		1993

[a] Data from ref 33. [b] Data from ref 13. [c] Data from ref 34.

determination could not be obtained. Complex **6** yielded crystalline material by slow diffusion of diethyl ether into a CH_2Cl_2 solution of the cluster. However, these crystals were either twinned or multiplet crystals. Changing the cation to $[PPN]^+$, $[BzMe_3N]^+$, or $[Ph_4As]^+$ did not produce single crystals, nor did the growing of the crystals by vapor diffusion or slow evaporation of the solvent. Complexes **7** and **8** exhibited similar complications. Although spectroscopic data indicate that these complexes contain organometallic fragments bound to the $\{W_6Cl_8\}^{4+}$ core via cyanide bridges and elemental analysis confirms their composition, an unambiguous establishment of their structures by X-ray diffraction eluded us.

Cluster **6** was prepared from **1** by reaction with $[Bu_4N][(C_5H_5)Mn(CO)_2(CN)]$ in moderate yield, and it exhibits IR bands at 2030 (ν_{CN}), 1918 (ν_{CO}), and 1865 cm^{-1} (ν_{CO}). These bands are shifted from those of $[Bu_4N][(C_5H_5)Mn(CO)_2(CN)]$: 2060 ($\nu_{CN}$), 1906 ($\nu_{CO}$), and 1831 cm^{-1} (ν_{CO}) (Table 8).[48] The cyanide-stretching frequency appears 30 cm^{-1} lower in energy in the bridged species relative to the unbridged complex. These frequencies are similar to those of the analogous molybdenum system $[Bu_4N]_2[Mo_6Cl_8\{(\mu\text{-}NC)Mn(CO)_2(C_5H_5)\}_6]$ (**10**),[13] which also exhibited a decrease in the ν_{CN} and an increase in both the ν_{CO} frequencies. The nitrogen atom of the cyanide ligands in **10** are bound to the Mo metal center, while the carbon atoms are bound to the Mn metal center. Thus, it is possible that the ligand disposition in **6** is the same as that of **10**.

Electrospray (ES^-) mass spectral data for **6**, Table 7, confirms the composition of this complex. A signal at $m/z = 1300$ agrees with the calculated value of 1300 for the dianion $[W_6Cl_8\{(\mu\text{-}NC)Mn(CO)_2(C_5H_5)\}_6]^{2-}$. An *R* factor (analogous to the crystallographic *R* factor) of 3.18 was determined using the peak intensities in the envelope ranging from $m/z = 1310-1290$. Five daughter ions are evident, which result from successive loss of $(C_5H_5)Mn(CO)_2$ fragments. In no case was the loss of a complete $(C_5H_5)Mn(CO)_2(CN)$ ligand observed. Apparently, the cyanide ligands remain attached to the cluster core, and the lowest molecular weight fragment observed is assigned to be $[W_6Cl_8(CN)_5\{(\mu\text{-}NC)Mn(CO)_2(C_5H_5)\}]^{2-}$, suggesting that the Mn−CN bond is cleaved more readily than the W−NC bond, as previously observed for the molybdenum cluster **10**.[13]

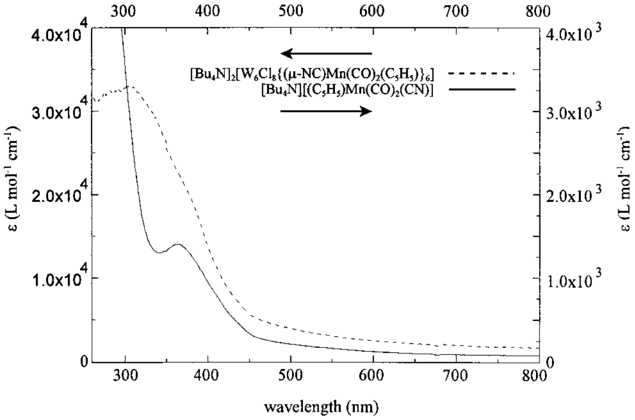

Figure 4. UV−vis spectra (overlay) of $[Bu_4N][(C_5H_5)Mn(CO)_2(CN)]$ (solid) and $[Bu_4N]_2[W_6Cl_8\{(\mu\text{-}NC)Mn(CO)_2(C_5H_5)\}_6]$ (**6**) (dashed) taken in CH_2Cl_2. The spectra are plotted on separate scales: $[Bu_4N][(C_5H_5)Mn(CO)_2(CN)]$ on the right and $[Bu_4N]_2[W_6Cl_8\{(\mu\text{-}NC)Mn(CO)_2(C_5H_5)\}_6]$ on the left.

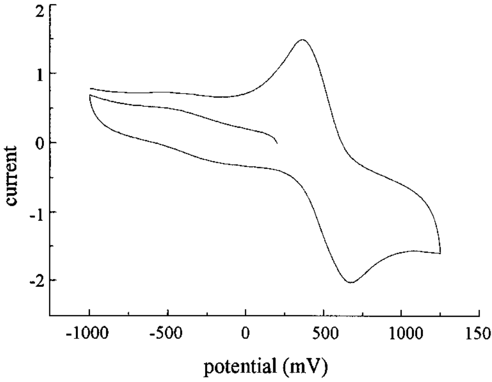

Figure 5. Cyclic voltammogram of $[Bu_4N]_2[W_6Cl_8\{(\mu\text{-}NC)Mn(CO)_2(C_5H_5)\}_6]$ (**6**). The initial potential is +200 mV, the initial sweep direction is negative, the maximum switching potential is +1250 mV, the minimum switching potential is −1000 mV, and the sweep rate is 100 mV s^{-1}.

Complex **7** is dark red in color, suggesting that charge-transfer bands occur between the Mn and W metal centers. The UV−vis spectrum of **6** shows one broad band with a λ_{max} of 308 nm ($\epsilon_{max} = 3.31 \times 10^4$ L mol^{-1} cm^{-1}), which is blue-shifted from that of $[Bu_4N][(C_5H_5)Mn(CO)_2(CN)]$ at 365 nm ($\epsilon_{max} = 7.10 \times 10^2$ L mol^{-1} cm^{-1}). An overlay plot of the UV−vis spectra for **6** and $[Bu_4N][(C_5H_5)Mn(CO)_2(CN)]$ is shown in Figure 4. The molar absorbtivity of **6** is much greater than that of the tosylate cluster **1** and of the uncoordinated manganese complex, indicating a charge-transfer transition, and vibronic coupling may also contribute to the high absorbtivity of **6**.[79,80] Examples of this type of coupling include octahedral transition-metal complexes, such as $IrBr_6^{3-}$ and $PtCl_6^{2-}$,[79] as well as the multiply bonded metal dimers $Mo_2Cl_4(PR_3)_4$ and $Re_2Cl_8$2-.[81] The position of λ_{max} for **6** moves to higher energy (lower wavelength) in CH_3CN relative to CH_2Cl_2 by 4 nm, which is consistent with a charge-transfer transition from the manganese cluster to the attached tungsten cluster.[39]

A cyclic voltammogram of **6** in CH_2Cl_2 (0.1 M in $[Bu_4N][BF_4]$) is shown in Figure 5. Compound **6** exhibits irreversible redox chemistry, with an oxidation wave at 672 mV, which may

---

(79) Fenske, R. F. *J. Am. Chem. Soc.* **1967**, *89*, 252.
(80) Lever, A. P. B. *Inorganic Electronic Spectroscopy*, 2nd ed.; Elsevier Science Publishers: Amsterdam, 1984.
(81) Hopkins, M. D.; Gray, H. B.; Miskowski, V. M. *Polyhedron* **1987**, *6*, 705.

correspond to the generation of $[W_6Cl_8\{(\mu\text{-NC})Mn(CO)_2(C_5H_5)\}_6]^{4+}$; the return wave occurs at 359 mV. The presence of a single wave indicates that the six manganese centers are electronically independent of one another. The oxidation potential of the free $[(C_5H_5)Mn(CO)_2(CN)]^-$ complex is 610 mV, and thus, it is reasonable to identify the manganese centers as the sites of oxidation.

Due to the irreversible behavior exhibited by **6**, a cell potential cannot be calculated. However, the oxidation wave at 672 mV is substantially shifted to more positive potential than that of $[Bu_4N][(C_5H_5)Mn(CO)_2(CN)]$ at 610 mV, suggesting that the ligands of **6** are harder to oxidize than the free complex. This also supports the argument that electron density is transferred from the manganese to the tungsten cluster.

Complex **6** is unstable to chemical oxidation. The analogous molybdenum cluster **10** undergoes clean oxidation by $[NO][PF_6]$ in acetonitrile to generate $[Mo_6Cl_8\{(\mu\text{-NC})Mn(CO)(NO)(C_5H_5)\}_6][PF_6]_4$, as shown by IR spectroscopy.[13] The oxidized product exhibits IR bands at 2128 (ν_{CN}), 2058 (ν_{CO}), and 1813 cm^{-1} (ν_{NO}). The shift in ν_{CN} to higher energy was expected, because the formal oxidation of the Mn atom by NO^+ reduces back-bonding from the Mn atom to the CN ligand. Although **6** does undergo reaction with $[NO][PF_6]$ under similar conditions, a clean product with the formula $[W_6Cl_8\{(\mu\text{-NC})Mn(CO)(NO)(C_5H_5)\}_6][PF_6]_4$ was not obtained. The cyanide-stretching frequency disappears, and removal of the solvent after reaction for 18 h resulted in the isolation of a dark oil, indicating extensive decomposition.

The neutral organometallic complexes $(C_5H_5)M(PPh_3)_2(CN)$ (M = Ru, Os) are sufficiently nucleophilic to displace the tosylate ligands from **1**. Reaction of these complexes with **1** produces **7** and **8**, which contain a 4+ cluster cation and four tosylate counterions. As observed for **6**, the position of the CN-stretching frequency in the IR spectrum of **7** and **8** shifts to lower energy relative to the free complexes upon coordination to the cluster (Table 8). These two clusters lack the intense color of **6**, and their UV−vis spectra do not indicate the presence of charge-transfer bands.

Conclusions

The tosylate cluster **1** may be prepared in high yield, and it can be used for the preparation of a variety of complexes containing the $\{W_6Cl_8\}^{4+}$ core. Cluster **1** is more stable in methanol and more stable to incoming basic ligands relative to **9**, so **1** can be used to prepare the pseudohalide clusters **2**, **3**, or **4** in higher yield than from **9**. Also, **1** can be used to prepare **5**, which is unavailable from **9**.

Cluster **1** can form complexes with organometallic axial ligands. The complex **6** was synthesized from **1** and was found to exhibit charge-transfer transitions. Complex **6** was characterized by spectrometric, spectroscopic, and electrochemical techniques. The clusters **7** and **8** were also prepared from **1**, but these two species appear to lack prominent charge-transfer transitions.

Acknowledgment. This research was supported by National Science Foundation Award CHE-9417250.

Supporting Information Available: X-ray crystallographic files in CIF format for the structure determinations of **1**, **4**, and **5**. This material is available free of charge via the Internet at http://pubs.acs.org.

IC001480Y